Influence of Ce_2O_3 addition on the basicity of Ni/MgO and on its catalytic performance in dry reforming of methane (Turning CO_2 to fuel)

تآثير اضافة آوكسيد السيريوم الثلاثي على قاعدية آوكسيد المغنيسيوم/نيكل وكذلك على فعاليته كعامل مساعد في تفاعل ثاني آوكسيد الكاربون مع الميثان. (تحويل غاز ثاني اوكسيد الكاربون الى وقود)

Faris A. J. Al-Doghachi[*], Yun Hin Taufiq-Yap[**]

[*]Department of chemistry, Faculty of science, University of Basrah, Basrah, Iraq.

[**]Department of Chemistry & Catalysis Science and Technology Research Centre, Faculty of Science, University Putra Malaysia, 43400 UPM Serdang, Selangor, Malaysia.

Abstract

The only way to stabilize the Earth's climate is to stabilize the concentration of greenhouse gases in the atmosphere. In this study, the conversion of methane and CO_2 to synthesis gas using dry reforming over catalysts $Ni/Mg_{1-X}Ce_XO$ (x= 0, 0.03, 0.07, 0.15; 1 wt% Ni each), dry reforming of methane was performed. The catalysts were prepared by K_2CO_3 co-precipitation from aqueous cerium nitrate hexahydrate and magnesium nitrate hexahydrate.

 Impregnation of nickel (II) acetylacetonate onto $MgO-Ce_2O_3$ was then conducted. TEM, XRD, FTIR, XRF, XPS, and BET characterizations of the catalysts were carried out. Results showed that the catalysts were reduced at 700 °C by H_2 prior to each reaction. CH_4 and CO_2 conversions at 900 °C of the catalysts after being tested for 200h decreased in the order $Ni/Mg_{0.85}Ce_{0.15}O$, $Ni/Mg_{0.93}Ce_{0.07}O$, $Ni/Mg_{0.97}Ce_{0.03}O$, and Ni/MgO. The highest H_2 and CO selectivities, was observed at a 1:1 CH_4:CO_2 mole ratio. We further performed a dry reforming in the presence of low-concentration oxygen flow (1.25 Vol %) and found an increased CH_4 conversion.

Keywords: Synthesis gas, H_2 production, Dry-Reforming of biogas, $MgO-Ce_2O_3$ catalyst

1- Introduction

Due to the current reliance on fossil fuels, the demand for energy has grown inevitably and so did the emission of some greenhouse gases especially carbon dioxide (CO_2). To prevent the negative outcome on climate change, the stabilization of the concentration of

such greenhouse gases in the atmosphere must be taken into consideration. However, with the economical development and the population growth, it is certain that energy will be one of the main issues in this century. In order to overcome these challenges, the provision of sustainable energy solutions is needed. Furthermore, the digestion of biomass anaerobically (fermented wastes) to produce biogas (CO_2 and CH_4) has been utilized as a fuel to produce power and heat. Also, it has been used as a renewable source of carbon in the production of synthesis gas (syngas: CO and H_2) for industrial feedstock through a reaction that is economical and environmental friendly [1]. One of the method to this process requiring intensive enegy, is the usuage of carbon dioxide as an oxidant known as the 'dry reforming process', as shown in eq (1).

$$CH_4 + CO_2 \rightarrow 2\,CO + 2H_2 \qquad \Delta H^{\circ}_{298K} = 247 kJ/mol \qquad (1)$$

Syngas is an important feedstock, that upon the usage of the Fischer-Tropsch synthesis can effectively be converted to fuels like gasoil, gasoline, methanol, and dimethyl ether (DME) [2]. However, varying the H_2/CO molar ratios is required in accor- dance with the industrial applications of syngas. For example, the H_2/CO ratio of 2 is required for methanol synthesis; [3] whilst the ratio is controlled at 1 for dimethyl ether (DME) synthesis under the single step process [4]. In the Fisher–Tropsch process, the H_2/CO ratio is usually in the range of 1 to 2, depending on the type of fuel synthesized [5]. Consequently, the H_2/CO ratio in syngas plays an important role in fuel production.

Simultaneous reverse water-gas shift (RWGS) reaction (eq (2)) affects the equilibrium of the reaction during the production of syngas from CH_4 and CO_2 (eq (1)). The resulting effect is a low H_2/CO ratio.

$$CO_2 + H_2 \rightarrow CO + H_2O \qquad \Delta H^{\circ}_{298K} = 41.0 \text{ kJ/mol} \qquad (2)$$

Other side reactions such as the decomposition of methane (eq (3)) and disproportionation reaction (Boudouard reaction) (eqn (4)) are also associated with the dry reforming reaction.

$$CH_4 \rightarrow C + 2H_2 \qquad \Delta H^{\circ}_{298K} = 75 kJ/mol \qquad (3)$$

$$2CO \rightarrow C + CO_2 \rightarrow CO_2 + C \quad \Delta H^{\circ}_{298K} = -172 kJ/mol \qquad (4)$$

133

Zhang et al. [6] demonstrated that the CH_4 decomposition (eq (3)) and CO disproportionation (eq (4)) were directly related to the deposition of carbon on the catalyst. Moreover, increasing the reaction's temperature from 550°C to 650°C, showed a greater tendency for the carbon deposition rather than the DRM. Thus, inorder to prevent the carbon formation and improve the DRM reaction, a careful choice of catalyst is crucial [6]. Furthermore, the support of metal in a metal oxide with strong basicity reduces the deposition of carbon and can even eliminate it [7]. This results due to the chemical adsorption of the support that causes the catalyst to chemisorb CO_2 in the CO_2 reforming of methane. Eventually, these species react with C to form CO (eq (5)).

$$CO_2 \ + \ C \ \rightarrow \ 2CO \qquad \Delta H°_{298K} = +172 \ kJ/mol \qquad\qquad (5)$$
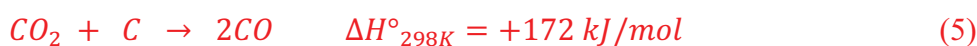
The use of nickel is highly recommended for the reforming process, as this active metal is readily available, inexpensive and due to its prevention of carbon formation. However, the main disadvantage of nickel is that it causes the formation of carbon that brings about catalytic deactivation rather easily [8]. Consequently, many research was conducted with the aim of improving the activities of catalysts and the stability of Ni catalysts in the reforming process [9]. When a strong Lewis base promoters, such as MgO or CaO were added, the Ni-based catalysts became deactivated. However, this can be improved with the chemisorbing of CO_2, to reduce the deposit of coke that reacts with deposited carbon to form carbon monoxide [10].

As such, the aim of research study is to prepare a catalyst with high selectivity, activity, and stability, as well as with the ability to decrease the deposits of carbon on the catalyst during the DRM reaction. The coprecipitation method included the precipitant K_2CO_3. Subsequently, the impregnation of 1% of Ni using nickel acetylacetonat, was carried out for the preparation of $Ni/Mg_{1-X}Ce_XO$ catalysts. Also, this research investigated the effects of the concentrations of CO_2 and CH_4 from natural gas or from biogas on the catalyst concentration and on the conversion temperature of the prepared catalysts in the DRM. Furthermore, this study attempted to evaluate the stability of the catalyst. This research study investigates the improvement in the conversion of methane for a stream of 1.25% O_2 gas passing through during the process.

2- Experimental

2.1 Support and catalyst preparation

In this work, the following catalysts were prepared, $Ni/Mg_{1-X}Ce_XO$ (x= 0, 0.03, 0.07, 0.15; 1 wt% Ni for each) through K_2CO_3 Table (1) co-precipitation from aqueous cerium nitrate hexahydrate and magnesium nitrate hexahydrate [11]. Following filtration and subsequent washing with warm water, the precipitate was dried for 12 h at 120 °C and pre-calcined at 500 °C in air for 5 h. The precipitate was pressed into disks at 600 kg/m^2 and calcined again at 1150 °C in air for 20 h. Afterwards, $Ni/Mg_{1-X}Ce_XO$ and Ni/MgO catalysts were prepared by impregnating a support comprising of a $Ni(C_5H_7O_2)_2 \cdot H_2O$ dichloromethane solution. After impregnation in air for 12 h, the obtained catalysts were dried at 120 °C.

Table (1) The description of materials

Material	Company	Purity (%)
$Ce(NO_3)_3.6H_2O$	Merck	99.0%
$Mg(NO_3)_2.6H_2O$	Merck	99.0%
K_2CO_3	Merck	99.7%
$Ni(C_5H_7O_2)_2 \cdot H_2O$	Acros Chemicals	99.%

2.2 Catalyst characterization

The catalysts synthesized were characterized by XRD, FTIR, BET, and TEM, and XPS. X-ray diffraction analysis was performed using a Shimadzu diffractometer model XRD 6000. The diffractometer employed Cu-Kα radiation to generate diffraction patterns from powder crystalline samples at ambient temperature. The Cu-Kα radiation was generated by Philips glass diffraction X-ray tube broad focus 2.7 kW type. The crystallite size D of the samples was calculated using the Debye-Scherrer's relationship [11], Where D is the crystalline size, λ is the incident X-ray wavelength, β is the full width at half-maximum (FWHM), and θ is the diffraction angle.

The Fourier transform infrared (FTIR) analysis was carried out with Perkin-Elmer spectrometer model 100 series (sample preparation UATR).

The total surface area of the catalysts was obtained using Brunauer-Emmett-Teller (BET) method with nitrogen adsorption at −196°C. Analysis was conducted using a

Thermo Fisher Scientific S.P.A (model: Surfer Analyzer) nitrogen adsorption–desorption analyzer.

The Transmission Electron Microscopy (TEM, Model Hitachi H7100, Japan) was used to determine the crystal shape and Homogeneity of the Catalysts. Briefly, in deionized water, the powder was dispersed, dropped on to the Carbon-cover copper grids placed on a filter paper and at room temperature dried.

XPS spectra were obtained using Kratos Axis Ultra DLD system, equipped with a mono-chromatic Al Kα (1486.6 eV), dual x-ray sources (Al & Mg), an argon etching system for sample cleaning and depth profiling, parallel imaging XPS, AES, ISS and Vision software for controlling the system. The base pressure of the analyzer chamber was 1×10^{-10}Torr. The excitation sources, X-ray gun was operated as a combination of 20 mA of emissions current and 15 kV voltages. The hemispherical analyzer was operated in the fixed analyzer transmission (FAT) mode for both wide and narrow scanning. This value is set at 100 eV and 40 eV of pass energy respectively. The region of interest for the narrow scan is corresponding to Mg2p, Ni2p, Ce3d, and O1s photoelectron signal.   The carbon charging correction refers to the binding energy of adventitious carbon at the binding energy of 285 eV. This highly sophisticated equipment is considered as a non-destructive analysis technique due to soft x-ray production to induce photoelectron emission from the sample surface. Therefore, the equipment would provide information about surface layers or thin film structures (about the top 10–100 Å of the sample).

2.3 Catalyst evaluation

Catalyst activity was evaluated for DRM in a continuous flow system by using a stainless-steel fixed-bed micro reactor (i.d. Ø = 6 mm, h = 34 cm), which was connected to the gas chromatography (GC) (Agilent 6890N; G 1540N) equipped with varian capillary columns HP-PLOT/Q and HP-MOLSIV and a mass-flow gas controller (SIERRA instrument) Figure (1). Before each reaction, about 0.02 g of catalyst was reduced by flowing 5% H_2/Ar (hydrogen diluted with inert gas argon) at a rate of 30 mL/min from 200 °C to 700 °C held for 3 h. Methane reforming was carried out by flowing a gas mixture comprising 2:1 and 1:1 CH_4:CO_2 at a rate of 30 mL/min from 700 °C to 900 °C at atmospheric pressure held for 200 h.
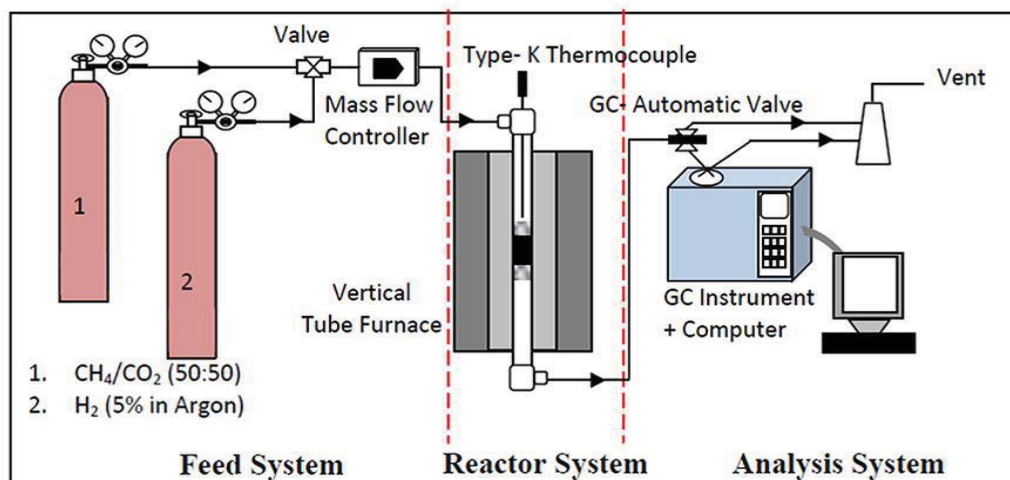
Fig. (1) Experimental system for dry reforming of methane.

3- Results and Discussions

3.1 Characterization of the Catalysts

3.1.1 XRD patterns

Figure 2 demonstrates the XRD patterns for the catalyst. The wide-angle XRD patterns of Ce_2O_3-MgO supported by nickel catalysts revealed MgO reflections. Diffraction peaks were observed at about $2\theta = 37.0$ (111), 42.9 (200), 62.3 (220), 74.7 (311) and 79.1° (222). This was due to the cubic form of magnesia (JCPDS file no.: 00-002-1207) [12]. Diffraction lines were found at about $2\theta = 28.6$ (111), 33.1 (200), 47.5 (220), 56.4 (311), 59.1 (222), 69.4 (400), 76.7 (331) and 79.1° (420) were due to the cubic form of ceria (JCPDS file no.: 00-034-0394). The peaks were recorded at $2\theta = 47.7$ (116), 56.5 (115), 59.3 (304), 62.5 (104), 69.7 (224), 77.0 (317), and 79.3° (318) were attributed to the cubic form of catalyst complex (Ce-Mg-O). However, there were no diffraction peaks for the catalyst of 1% nickel in all the patterns. This was because the amount of these elements was very small.We also determined that the catalysts were in the cubic phase based on their crystal system, as indicated by the image of TEM as shown in Figures (2, 3).
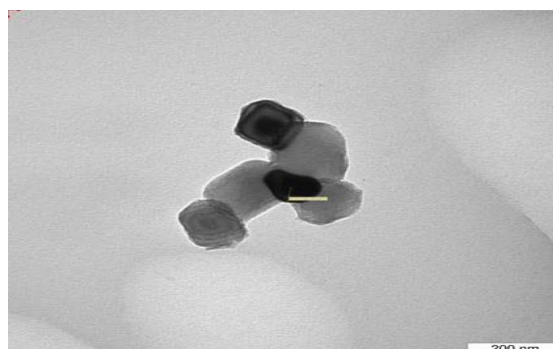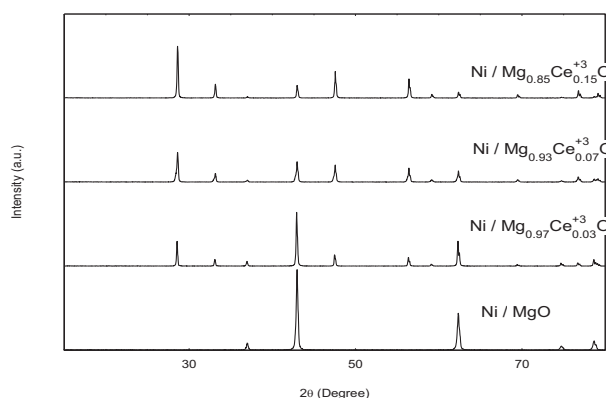
Fig. (2) XRD patterns of the catalysts   **Fig. (3) TEM image for Ni/Mg$_{0.85}$Ce$_{0.15}$O**

3.1.2 FTIR & XPS

The measurement of the FTIR reveal that the Ni-O, Ce-O, and MgO bonds were present in the far-IR region, and all spectrum peaks were due to acetylacetonate. Figures 4(a-d) demonstrate photoelectron signals from Ni2p, O1s, CeO and Mg2p as determined by the XPS data of the few top most nanometer layers on the catalyst surface. Four oxygen species [O^{2-} (from the bulk), CeO, MgO, and NiO contributed the O1s photoelectron signal [12]. This splitting was also attributed to the significant splitting of O1s spectrum, in which NiO had the highest photoelectron-signal intensity at the low-binding-energy region. We detected O^{2-}, CeO, NiO, and OH^{-} under a similar photoelectron envelope, but the contribution of OH^{-} was deemed to be very low at 533.0 eV binding energy. Furthermore, the oxide species of these metals were a mixture of MgO and Mg(OH)$_2$, CeO and Ni(OH)$_2$, and NiO as revealed by a narrow scan of Mg2p, Ce3d, and NiO, respectively [13].

138
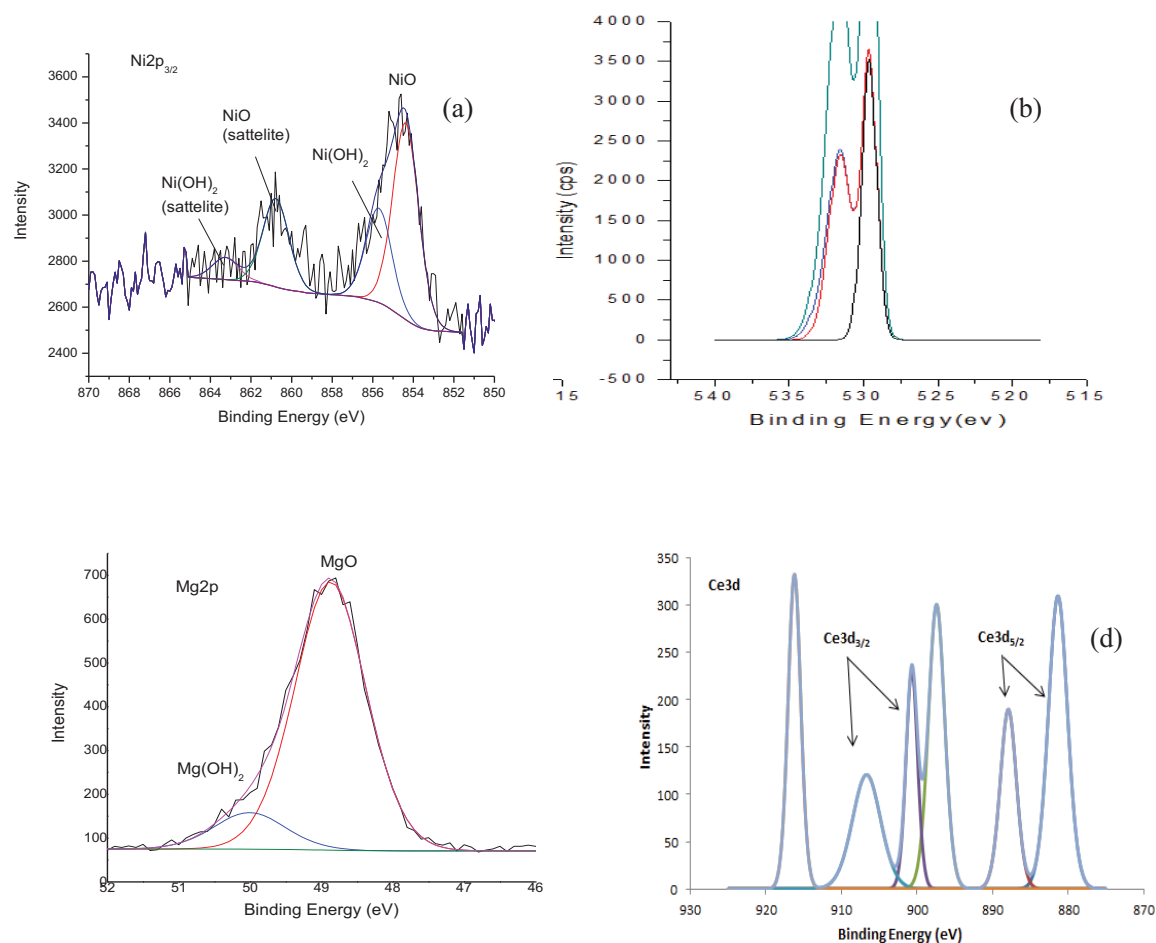
Fig. (4) XPS of the Ni/Mg$_{1-X}$Ce$_X$O catalyst.

Table (2) shows the values of BET specific surface area (S_{BET}) and the pore properties of catalyst supports and freshly prepared catalysts. The S_{BET} values increased and the pore properties deteriorated in all three catalysts after impregnation, which may be due to pore blocking during impregnation [14].

Table (2) The main textural properties of fresh catalysts.

Sample name	Specific [a] Surface Area m^2/g	Pore Volume cm^3/g	Pore radius Å	Ni [b] Loading wt %	Average [c] Crystal size nm
Ni/ MgO	6.07	0.11	28.40	0.97	38.7
Ni/Mg$_{0.97}$Ce$_{0.03}$O	8.61	0.03	23.23	0.88	42.11
Ni/Mg$_{0.93}$Ce$_{0.07}$O	9.82	0.05	18.23	0.92	44.67
Ni/Mg$_{0.85}$Ce$_{0.15}$O	10.66	0.21	30.82	0.93	40.41

a. Specific surface area calculated by BET method.

b. Determined by the XRF method.

c. Determined by the Debye-Scherrer equation of the Mg (200) plane of XRD.

Table (2) also presents the S_{BET} values, pore volumes, and average Ni-loadings of our prepared catalysts. Ni/Mg$_{0.85}$Ce$_{0.15}$O had the largest pore volume and S_{BET} value [15], respectively. No obvious relationship was found between the S_{BET} value and pore volume of catalysts, but the S_{BET} increased in the order of Ni/MgO < Ni/Mg$_{0.97}$Ce$_{0.03}$O < Ni/Mg$_{0.93}$Ce$_{0.07}$O < Ni/Mg$_{0.85}$Ce$_{0.15}$O. This result was consistent with the Ni-dispersion order, due to a big size of Ce atom.

Aldoghachi *et al.* [12] studied high surface area showed that it contributed to high catalyst performance. Table (2) shows the XRF results, in which Ni loading was found to be ≤ 1%. This finding may be due to the loss of weight during support pre-calcination, thereby resulting in a high Ni content of catalysts.

3.1.3 Thermogravimetric analysis

Figure (5) shows the TGA analysis for the reduced catalysts: Ni/MgO, Ni/Mg$_{0.97}$Ce$_{0.03}^{3+}$O, Ni/Mg$_{0.93}$Ce$_{0.07}^{3+}$O, and Ni/Mg$_{0.85}$Ce$_{0.15}^{3+}$O. The results revealed that there was a weight loss at only one stage for all the catalysts. The estimated weight loss, which was approximately 1.5%, occurred in the temperature range between 100 °C and 150 °C. This can be attributed to the removal of moisture from the Ni/Mg$_{1-x}$Ce$_x$O catalysts.

The estimated weight losses for Ni/MgO, Ni/Mg$_{0.93}$Ce$_{0.07}^{3+}$O, Ni/Mg$_{0.97}$Ce$_{0.03}^{3+}$O, and Ni /Mg$_{0.85}$Ce$_{0.15}^{3+}$O catalysts were recorded to be 1.3%, 1.2%, 1.8% and 1.7%, respectively. There was a slight initial increase due to the adsorption of the N$_2$ gas on the compound. All the compounds became thermally stable at 500 °C, which corresponds to the high melting points of magnesia and ceria at 2852 °C and 2177 °C, respectively. This also helps in establishing good interaction among the components of the catalyst. The findings of the thermal analysis were similar and consistent with the results of Mojovic et al. [16].
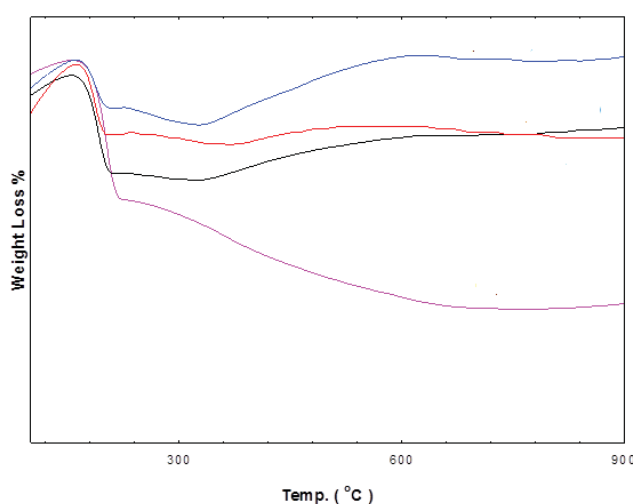
Fig. (5) TGA of the catalysts (a) Ni/MgO (b) Ni/Mg$_{0.93}$Ce$_{0.07}^{3+}$O (c) Ni/Mg$_{0.97}$Ce$_{0.03}^{3+}$O (d) Ni/Mg$_{0.85}$Ce$_{0.15}^{3+}$O.

3.2 Catalytic performance in biogas reforming

Catalyst activity in DRM was indicated by CH$_4$ and CO$_2$ conversion. H$_2$/CO ratio was used to express selectivity. The most active catalyst in DRM of biogas is shown in figure (6). After the reaction proceeded for 200 h at 900 °C, the catalyst yielded 98% and 84% conversion for both CO$_2$ and CH$_4$, respectively, and the H$_2$/CO ratio was 1.24. CO$_2$ and CH$_4$ conversion decreased in the order of Ni/Mg$_{0.85}$Ce$_{0.15}$O > Ni/Mg$_{0.93}$ Ce $_{0.07}$O > Ni /Mg$_{0.97}$ Ce $_{0.03}$O > Ni/MgO. Carbon formation may have had the highest resistance of deactivation, and thus the highest H$_2$ and CO selectivities, were observed in 1:1 CH$_4$:CO$_2$

mole ratio [17]. BET results indicated that crucial to the conversion process were the pore size of supporter and doping metal. DRM of the biogas reaction was further performed in the presence of low-concentration oxygen (1.25%) flow, and enhanced the conversion of CH_4 from 84 to 96%, results are shown in Figure (7). Initially, the reaction of this oxygen with methane to give CO and H_2O eq. (6), thus, the syngas formed from their produced steam with the carbon deposition (eq. (7)).

$$CH_4 + 1.5O_2 \rightarrow CO + 2H_2O \qquad (6)$$
$$C(s) + H_2O \rightarrow CO + H_2 \qquad (7)$$

Table (1) shows that with an increase in the concentration of Ce_2O_3, there was an increase in the surface area from the BET result. The best result observed by the catalyst $Ni/Mg_{0.85}Ce_{0.15}O$ was found at the conversion rate of CH_4 and CO_2 as well as the ratio of H_2/CO This phenomenon reveals that the incorporation of Ce_2O_3 into the MgO catalysts can significantly depress the Reverse Water Gas Shift (RWGS) reaction (eq. 2) [18].

DRM reaction has been investigated and comparison of noble (Rh, Ru, Pd, Ir and Pt) and non-noble (Ni and Co) metal catalysts was made by Tsyganok et al. [19] and reported that the Ni and Co catalysts showed higher catalytic activities compared to the noble metal supported catalysts. However, the higher coke depositions of Ni and Co catalysts indicated their poor coke resistance ability compared to noble metal catalysts [20]. Thus, the deactivation arising from the coke deposition is the major obstacle in the application of Ni-based catalyst. As a result of this process the carbon deposition is reduced and consequently the lifetime of the catalyst could be improved using $Ni/Mg_{1-x}Ce_xO$ catalysts.
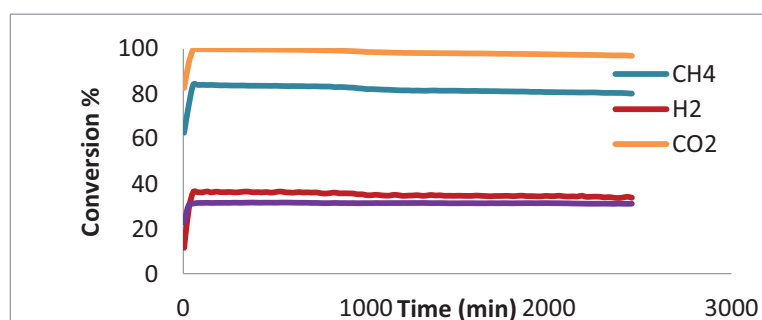
Fig. (6) Stability tests of Ni/Mg0.85Ce0.15O fresh catalysts (a) and recycled catalysts at 900°C for 200 h (GHSV = 15000 ml cat-1h-1, atmospheric pressure).
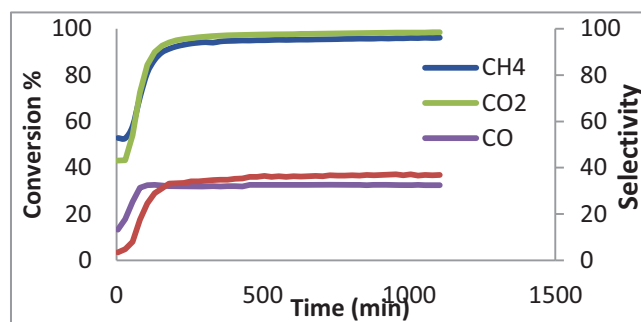
**Fig. (7) DRM reaction of the Ni/Mg0.85Ce0.15O catalyst
under 900°C with 1.25% O2**

Post-reaction characterization

The image of TEM and TGA analysis detected the presence of a coke deposit with an oxygen stream of spent catalyst. Figure (8) illustrates the TEM images. The image shows that the original structure of the catalyst was maintained even after 200h of stream testing. Furthermore, the spent catalyst kept its two-dimensional cubic texture. The phenomenon of a slight metal sintering was observed in the spent catalyst. Whilst the two-dimensional cubic channel of spent catalyst limited the sintering of the active metals inside the pore, the active metals supported on the outside surface experienced significant sintering. Since no filamentous carbon was found in the spent catalyst, it can be concluded that the coke deposition was negligible [12].
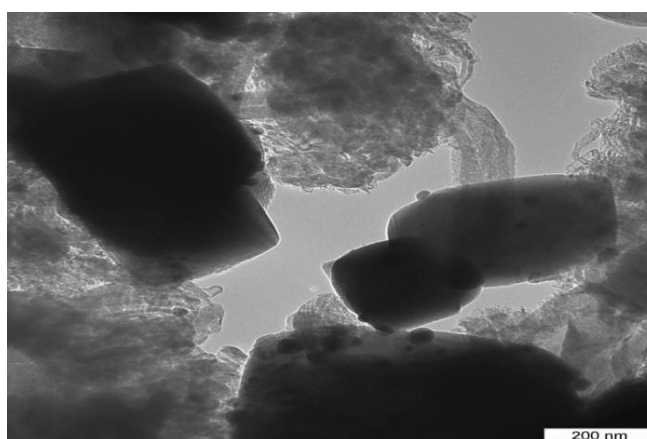
Fig. (8) Ni/Mg$_{0.85}$Ce$_{0.15}$O after 200h reaction, at 900°C, and CH$_4$/CO$_2$ ratio 1:1.

4. <u>Conclusion</u>

Dry reforming of methane over Ni/Mg$_{1-x}$Ce$_x$O catalysts was carried out for the production of syngas. The catalysts were synthesized using co-precipitation method and subsequently pre-screened by testing the catalytic performance in methane dry reforming reaction.

The pre-screening test showed that Ni/Mg$_{0.85}$Ce$_{0.15}$O catalyst has the best catalytic performance in terms of conversion and yield. Hence, Ni was selected as the active metal to be dispersed on the Mg$_{0.85}$Ce$_{0.15}$O support. The interaction effects of factors such as concentration metals support, reactant (CH$_4$:CO$_2$) ratios (1:1 and 2:1) and reaction temperature (700-900°C) were considered in the performance of the Ni/Mg$_{0.85}$Ce$_{0.15}$O in terms of CH$_4$ and CO$_2$ conversion as well as H$_2$ and CO yield. The Ni/Mg$_{0.85}$Ce$_{0.15}$O catalyst showed a promising performance at reaction temperature of 900 °C and CH$_4$:CO$_2$ ratios at 1:1 with highest CH$_4$ and CO$_2$ conversions of 83% and 99% respectively. The Ni/Mg$_{0.85}$Ce$_{0.15}$O catalyst was subsequently characterized for its physicochemical properties by XRD, FTIR, TEM, EDX, BET and XPS. The methane dry reforming over the Ni/Mg$_{0.85}$Ce$_{0.15}$O gave syngas ratio of 1.2 making it suitable for production of oxygenated fuel via Fischer-Tropsch synthesis. The reaction was further performed in the presence of low-concentration oxygen (1.25%) and enhanced the conversion of CH$_4$ from 83 to 95%.

References

1. D. C. Carvalho, H. S. Souza, M. Josu⁄e Filho, E. M. Assaf, V. V. Thyssen, A. Campos and A. C. Oliveira, (2014), Synthesis, characterization and biological evaluation of cationic hydrazone copper complexes with diverse diimine co-ligands *RSC Adv.,* 4, 61771–61780.

2. Gonzalez, R. G. (2006), Fischer-Tropsch and GTL update. *Petroleum Technology Quarterly*, 11(2), 60-80.

3. M. R. Rahimpour, Z. A. Aboosadi and A. H. Jahanmiri (2011), Optimization of tri-reformer reactor to produce synthesis gas for methanol production using differential evolution (DE) method, *Appl. Energy*, 88, 2691-2701.

4. W. H. Chen, B. J. Lin, H. M. Lee and M. H. Huang (2012), One- step synthesis of dimethyl ether from the gas mixture containing CO_2 with high space velocity, *Appl. Energy*, 98, 92–101.

5. M. Sarkari, F. Fazlollahi, H. Ajamein, H. Atashi, W. C. Hecker and L. L. Ba xter, (2014), Catalytic performance of an iron-based catalyst in Fischer – Tropsch synthesis, *Fuel Process. Technol.,* , 127, 163–170.

6. J. Zhang, H. Wang and A. K. Dalai, (2007), Development of stablebimetallic catalysts for carbon dioxide reforming of methane. *Journal of Catalysis*, 249(2), 300-310.

7. Z. L. Zhang, and X. E. Verykios, (1994), Carbon dioxide reforming of methane to synthesis gas over supported Ni catalysts. *Catalysis Today* 21(2-3), 589-595.

8. J. Ashok, and S. Kawi (2013), Steam reforming of toluene as a biomass tar model compound over CeO_2 promoted $Ni/CaO-Al_2O_3$ catalytic systems, *International journal of hydrogen energy* 38(32) 13938-13949.

9. Y. Liu, Z. He, L. Zhou, Z. Hou, and W. Eli, (2013), Simultaneous oxidative conversion and CO_2 reforming of methane to syngas over Ni/vermiculite catalysts *Cataly Communications*, 42, 40-44.

10. Q. J. Chen, J. Zhang, Q. W. Jin, B. R. Pan, W. B. Kong, T. J. Zhao, and Y. H. Sun, (2013) Effect of reflux digestion treatment on the catalytic performance of Ni-$CaO-ZrO_2$ nanocomposite catalysts for CO_2 reforming of CH_4 *Catalysis today* 215, 251-259.

11. F. A. Al-Doghachi, U. Rashid and Y. H. Taufiq-Yap, (2016), Investigation of Ce (III) promoter effects on the tri-metallic Pt, Pd, Ni/MgO catalyst in dry- reforming of methane. *RSC Advances* 6 (13), 10372-10384.

12. F. A. Al-Doghachi, A. Islam, Z. Zainal, M. I. Saiman, Z. Embong, and Y. H. Taufiq-Yap, (2016), High Coke-Resistance $Pt/Mg_{1-x}Ni_xO$ Catalyst for Dry Reforming of Methane *PloS one* 11(1) e0145862.

13. E. Ruckenstein and Y. H. Hu (2000), Catalytic Conversion of Methane to Synthesis Gas by Partial Oxidation and CO_2 Reforming, *Chem. Innovation*, 30, 39-43.

14. B. Saha, A. Khan, H. Ibrahim and R. Idem (2014), Evaluating the performance of non- precious metal based catalysts for sulfur- tolerance during the dry reforming of biogas, *Fuel*, , 120, 202–217.

15. B. Saha, A. Khan, H. Ibrahim and R. Idem, (2014), Evaluating the performance of non-precious metal based catalysts for sulfur-tolerance during the dry reforming of biogas *Fuel,* 120, 202-217.

16. Z.Mojovic,S.MentusandZ.Tesic(2004), Introduction of Pt and Pd Nanoclusters in Zeolite Cavities by Thermal Degradation of Acetylacetonates, *Mater. Sci. Forum*, 453, 257–263.

17. F. A. Al-Doghachi, U. Rashid, Z. Zainal, M. I. Saiman and Y. H. Taufiq Yap, (2015) Influence of Ce_2O_3 and CeO_2 promoters on Pd/MgO catalysts in the dry-reforming of methane, *RSC Advances* 5(99), 81739-81752.

18. J. Kehres and Jakobsen(2012), Dynamical Properties of a $Ru/MgAl_2O_4$ Catalyst during Reduction and Dry Methane Reforming, *J. Phys. Chem. C,* 116, 12407-21415.

19. A, I. Tsyganok, M. Inaba, T. Tsunoda, S. Hamakawa, K. Suzuki and T. Hayakawa, (2003) Dry reforming of methane over supported noble metals: a novel approach to preparing catalysts *Catal. Commun*. 4(9) 493–498.

20. J. Rostrupnielsen, J. Hansen (1993), CO_2 reforming of methane over transition metals. Journal of Catalysis, 144, 38-49.